





Article

Structure–Activity Relationship of Pyrrolidine Pentamine Derivatives as Inhibitors of the Aminoglycoside 6'-N-Acetyltransferase Type Ib

Jan Sklenicka¹, Tung Tran¹, Maria S. Ramirez¹ , Haley M. Donow², Angel J. Magaña¹, Travis LaVoi², Yasir Mamun^{3,4}, Verónica Jimenez¹ , Prem Chapagain^{3,4} , Radleigh Santos⁵, Clemencia Pinilla⁶, Marc A. Giulianotti⁶ and Marcelo E. Tolmasky^{1,*} 

- ¹ Center for Applied Biotechnology Studies, Department of Biological Science, College of Natural Sciences and Mathematics, California State University Fullerton, Fullerton, CA 92831, USA; jsklenicka@csu.fullerton.edu (J.S.); tungtran6186@yahoo.com (T.T.); msramirez@fullerton.edu (M.S.R.); angelmagana@fullerton.edu (A.J.M.); vjimenezortiz@fullerton.edu (V.J.)
- ² Center for Translational Science, Florida International University, Port St. Lucie, FL 34987, USA; hmdonow@gmail.com (H.M.D.); tlavoi@fiu.edu (T.L.)
- ³ Department of Physics, Florida International University, Miami, FL 33199, USA; ymamun001@fiu.edu (Y.M.); chapagain@fiu.edu (P.C.)
- ⁴ Biomolecular Sciences Institute, Florida International University, Miami, FL 33199, USA
- ⁵ Department of Mathematics, Nova Southeastern University, Fort Lauderdale, FL 33314, USA; radleigh@nova.edu
- ⁶ Department of Medicinal Chemistry and Institute for Translational Neuroscience, University of Minnesota, Minneapolis, MN 55455, USA; pinil005@umn.edu (C.P.); giuli050@umn.edu (M.A.G.)
- * Correspondence: mtolmasky@fullerton.edu; Tel.: +1-657-278-5263



Citation: Sklenicka, J.; Tran, T.; Ramirez, M.S.; Donow, H.M.; Magaña, A.J.; LaVoi, T.; Mamun, Y.; Jimenez, V.; Chapagain, P.; Santos, R.; et al. Structure–Activity Relationship of Pyrrolidine Pentamine Derivatives as Inhibitors of the Aminoglycoside 6'-N-Acetyltransferase Type Ib. *Antibiotics* **2024**, *13*, 672. <https://doi.org/10.3390/antibiotics13070672>

Academic Editor: Marc Maresca

Received: 20 May 2024

Revised: 9 July 2024

Accepted: 17 July 2024

Published: 19 July 2024



Copyright: © 2024 by the authors. Licensee MDPI, Basel, Switzerland. This article is an open access article distributed under the terms and conditions of the Creative Commons Attribution (CC BY) license (<https://creativecommons.org/licenses/by/4.0/>).

Abstract: Resistance to amikacin and other major aminoglycosides is commonly due to enzymatic acetylation by the aminoglycoside 6'-N-acetyltransferase type I enzyme, of which type Ib [AAC(6')-Ib] is the most widespread among Gram-negative pathogens. Finding enzymatic inhibitors could be an effective way to overcome resistance and extend the useful life of amikacin. Small molecules possess multiple properties that make them attractive for drug development. Mixture-based combinatorial libraries and positional scanning strategy have led to the identification of a chemical scaffold, pyrrolidine pentamine, that, when substituted with the appropriate functionalities at five locations (R1–R5), inhibits AAC(6')-Ib-mediated inactivation of amikacin. Structure–activity relationship studies have shown that while truncations to the molecule result in loss of inhibitory activity, modifications of functionalities and stereochemistry have different effects on the inhibitory properties. In this study, we show that alterations at position R1 of the two most active compounds, **2700.001** and **2700.003**, reduced inhibition levels, demonstrating the essential nature not only of the presence of an S-phenyl moiety at this location but also the distance to the scaffold. On the other hand, modifications on the R3, R4, and R5 positions had varied effects, demonstrating the potential for optimization. A correlation analysis between molecular docking values (ΔG) and the dose required for two-fold potentiation of the compounds described in this and the previous studies showed a significant correlation between ΔG values and inhibitory activity.

Keywords: aminoglycoside resistance; structure–activity relationship; aminoglycoside-modifying enzymes; acetyltransferase; Acinetobacter; small molecule inhibitor

1. Introduction

Multidrug resistance is one of the top concerns for human health. A growing number of people are dying due to acquiring resistant infections. At the same time, the multidrug resistance crisis has caused the cost of treatment to skyrocket [1–4], further compounding the issue. The number of new antimicrobials being developed falls short of what would be necessary for effectively managing the problem [5,6]. Furthermore, only one of the

recently approved antibiotics, cefiderocol, can be used against a bacterium included in the WHO list of critical pathogens [5]. Therefore, repurposing or extending the useful life of existing antimicrobials is essential to increase the armamentarium against the growing number of multidrug-resistant bacterial pathogens [7]. Aminoglycoside antibiotics have been an instrumental component of the armamentarium in treating life-threatening infections [8,9]. However, their spectrum of action is being diminished by the rise in resistance, mainly due to enzymatic modification catalyzed by aminoglycoside-modifying enzymes (AMEs) [8,10–12]. Significant efforts focused on designing new semisynthetic aminoglycosides by altering those found in nature to produce molecules refractory to the action AMEs [11,13]. While these efforts have resulted in the introduction of novel aminoglycosides like amikacin or plazomicin, attempts to identify or design inhibitors of the inactivating action of AMEs have been limited [11,12,14,15]. Consequently, no inhibitor has yet been introduced at the clinical level. Finding one suitable for human use will permit the design of effective combination therapies against resistant bacteria, thus extending the useful life and scope of existing aminoglycosides [7].

Amikacin is an aminoglycoside of high clinical relevance, but resistance—usually caused by the action of the aminoglycoside 6'-N-acetyltransferase type Ib [AAC(6')-Ib]—abundant in numerous geographical regions [11,12,16,17]. Recent efforts to produce inhibitors of resistance mediated by this enzyme include exploring antisense strategies to turn off the expression of the *aac(6')-Ib* gene and the identification of various chemicals that interfere with the acetylation reaction [14,18–24]. In particular, small molecule inhibitors have the potential to serve as inhibitors of enzyme-mediated antibiotic resistance [25–27]. Developing an inhibitor that can be combined with amikacin could be an option to treat infections caused by multidrug-resistant strains that can no longer be controlled by carbapenems or other antimicrobials [20].

A recent study using mixture-based combinatorial libraries and the positional scanning strategy [28] identified a substituted pyrrolidine pentamine as a promising inhibitor of AAC(6')-Ib-mediated acetylation of amikacin and other aminoglycosides [22] (Figure 1A and Table 1). However, recent work has revealed that some bacterial strains produce AAC(6')-Ib in quantities far exceeding those needed for clinical resistance [16,29]. This finding highlights the necessity for an inhibitor with enough potency to effectively combat a range of pathogenic bacteria, even in environments with high enzyme concentrations. In addressing this challenge, we conducted further structure–activity relationship (SAR) studies to investigate how changes in the compounds' stereochemistry and substitutions of functionalities impact their inhibitory effectiveness [23]. Expanding upon our previous SAR analyses, this work aims to continue exploring the connection between molecular modifications and their inhibitory effects. Such insights are instrumental for designing a potent inhibitor that, in combination with amikacin, could overcome the resistance conferred by AAC(6')-Ib.

Table 1. Comparison of properties of compounds from different synthesis batches.

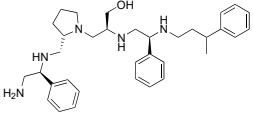
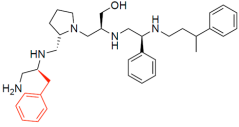
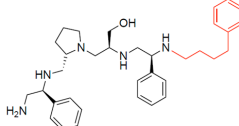
Compound		Growth Inhibition (%) ¹	SEM	Checkerboard Analysis Compound Concentration for Potentiation (μM)			
				2-Fold		3-Fold	
Structure	ID			50%	80%	50%	80%
	2637.001	60	4	3.0	4.2	6.7	9.4
R1: S-phenyl R2: S-pyrrolidine R3: S-hydroxymethyl R4: S-phenyl R5: 3-phenylbutyl	2700.001	52	4	6.5	10.4	8.8	12.9

Table 1. Cont.

Compound	Structure	ID	Growth Inhibition (%) ¹	SEM	Checkerboard Analysis Compound Concentration for Potentiation (μM)			
					2-Fold		3-Fold	
					50%	80%	50%	80%
		2637.003	20	3	N.D.	N.D.	N.D.	N.D.
	R1: S-benzyl R2: S-pyrrolidine R3: S-hydroxymethyl R4: S-phenyl R5: 3-phenylbutyl	2700.002	19	4	N.D.	N.D.	N.D.	N.D.
		2637.011	66	6	8.3	8.9	11.6	12.5
	R1: S-phenyl R2: S-pyrrolidine R3: S-hydroxymethyl R4: S-phenyl R5: 4-phenylbutyl	2700.003	53	9	7.2	10.0	8.9	12.2

SEM, standard error of the mean; N.D., not determined. ¹ Growth inhibition measured at 16 μg/mL amikacin and 8 μM of the test compound. Modifications to the compound 2700.001 are shown in red.

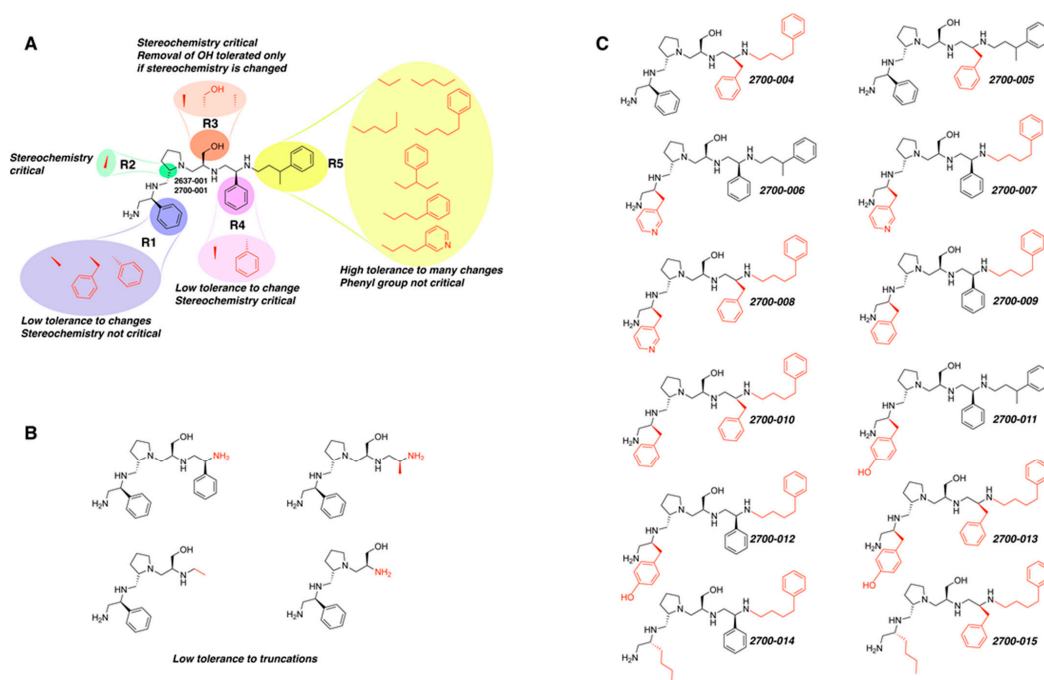


Figure 1. Compounds structures. (A) Chemical structure of compound 2700.001 (formerly 2637.001) showing the pyrrolidine pentamine scaffold with the two S-phenyl groups (blue and purple background), the S-hydroxymethyl group (orange background), and the 3-phenylbutyl group (yellow background) at the positions R1, R3, R4, and R5, respectively. Substitutions previously evaluated are shown in red over the corresponding color background. (B) Compounds resulting from truncations of various sizes to 2700.001. (C) Chemical structures of compounds assessed in this work. Substitutions with respect to 2700.001 are shown in red.

2. Results

The high relevance of AAC(6′)-Ib as the cause of resistance to amikacin in pathogenic Gram-negatives motivated the search for inhibitors of the enzymatic acetylation that inactivates the aminoglycoside molecule. Utilizing mixture-based combinatorial libraries and the positional scanning strategy, we identified compound **2637.001**, which consists of a pyrrolidine pentamine scaffold with two *S*-phenyl groups, an *S*-hydroxymethyl group, and a 3-phenylbutyl group at positions R1, R3, R4, and R5, respectively, as shown in Figure 1A. To study the potential interactions of compound **2637.001** with the AAC(6′)-Ib molecule and its inhibitory activity, a series of compound **2637.001** analogs were analyzed. Figure 1A,B graphically show the tolerance and effects of substituting the chemical groups at each location, modifying the stereochemical conformation at R2, or reducing the size of the molecule. Position R1 showed a low tolerance to modifications, including changing the stereochemistry, replacing the phenyl with a methyl group, and increasing the distance between the phenyl group and the scaffold.

Position R4 exhibited low tolerance to modifying the stereochemistry or replacing the phenyl with a methyl group. To gain further insights into the contribution or effect of substitutions at these positions in combination with substitutions at the R5 position, which has high tolerance to modifications, we generated a collection of twelve analogs with modifications at positions R1, R4, and R5 (Figure 1C, identified as **2700** series). The R1 location was unmodified or modified to carry a heteroatom in the aromatic moiety, to increase the distance between the phenyl or pyridine groups and the scaffold, or to replace the aromatic moiety with an aliphatic one that occupies approximately the same space. The R4 position was unmodified or modified to move the phenyl group away from the scaffold by inserting a methylene moiety. The R5 position was unmodified or modified by replacing the 3-phenylbutyl with a 4-phenylbutyl group.

Each compound's efficacy as an amikacin resistance inhibitor was evaluated on *A. baumannii* A155, a strain harboring the *aac(6′)-Ib* gene, at concentrations of 16 µg/mL amikacin and 8 µM of the test compound. Previous results showed that *A. baumannii* A155 can grow in 16 µg/mL amikacin containing Mueller–Hinton broth [23]. The growth curves of the cultures were determined by measuring OD₆₀₀ every 20 m, and the values after a 20 h incubation, when the cultures were already in stationary phase, were used to calculate the percentage of growth inhibition with respect to bacteria growing in media with the sole addition of amikacin.

To ensure that the results obtained with compounds synthesized at different times could be compared, an experiment was carried out to determine the inhibition levels of three compounds synthesized first for the previous study [23] and then for the present study (**2637.001**, now **2700.001**; **2637.003**, now **2700.002**; **2637.011**, now called **2700.003**). Comparisons were carried out at a single dose and using checkerboard assays for higher accuracy in the case of the two structures that showed more potent inhibition of amikacin resistance. The results of these tests are shown in Table 1. The inhibition levels observed when using compounds from both series were sufficiently close to confirm that the results obtained with the most recently designed compounds can be compared to the previous analyses.

Considering the features of the two compounds with higher inhibiting activity (**2700.001** and **2700.003**), a collection of analogs was generated to gain deeper insights into the effect of modifications at different positions. Inspection of the inhibition of amikacin resistance exerted by these compounds showed that one out of the twelve newly designed analogs, **2700.004**, appeared to restore resistance to amikacin at levels comparable to compounds **2700.001** and **2700.003** (Table 2).

Table 2. Properties of 2700.001 analogs.

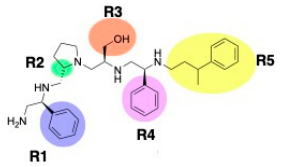
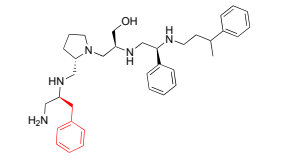
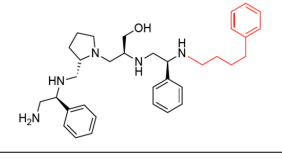
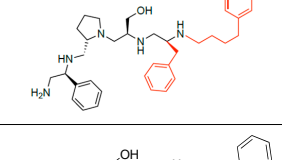
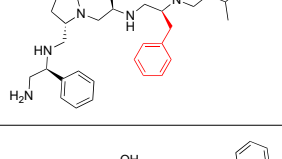
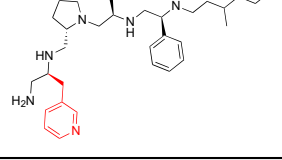
Compound		Functionalities					%Inhibition (Average, n = 8)	Standard Error
ID	Structure	R1	R2	R3	R4	R5		
2700.001 2637.001		S-phenyl	S-pyrrolidine	S-hydroxymethyl	S-phenyl	3-phenylbutyl	50	4
2700.002 2637.003		S-benzyl	S-pyrrolidine	S-hydroxymethyl	S-phenyl	3-phenylbutyl	19 **	4
2700.003 2637.011		S-phenyl	S-pyrrolidine	S-hydroxymethyl	S-phenyl	4-phenylbutyl	53	9
2700.004		S-phenyl	S-pyrrolidine	S-hydroxymethyl	S-benzyl	4-phenylbutyl	46	14
2700.005		S-phenyl	S-pyrrolidine	S-hydroxymethyl	S-benzyl	3-phenylbutyl	21 **	3
2700.006		S-3-methylpyridine	S-pyrrolidine	S-hydroxymethyl	S-phenyl	3-phenylbutyl	14 **	2

Table 2. Cont.

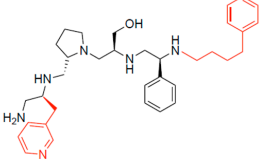
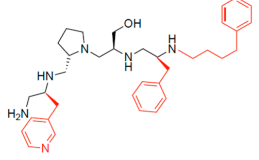
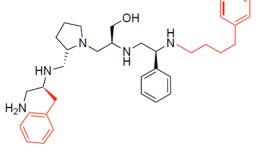
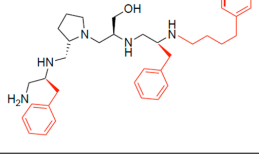
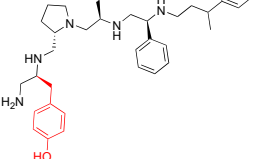
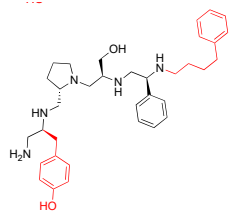
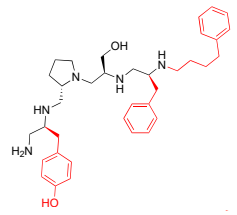
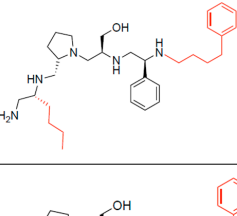
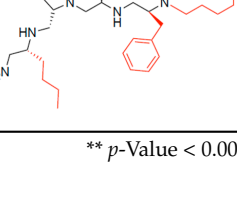
ID	Compound Structure	Functionalities					%Inhibition (Average, n = 8)	Standard Error
		R1	R2	R3	R4	R5		
2700.007		S-3-methylpyridine	S-pyrrolidine	S-hydroxymethyl	S-phenyl	4-phenylbutyl	14 **	2
2700.008		S-3-methylpyridine	S-pyrrolidine	S-hydroxymethyl	S-benzyl	4-phenylbutyl	11 *	3
2700.009		S-benzyl	S-pyrrolidine	S-hydroxymethyl	S-phenyl	4-phenylbutyl	12 **	3
2700.010		S-benzyl	S-pyrrolidine	S-hydroxymethyl	S-benzyl	4-phenylbutyl	23 *	7
2700.011		S-4-hydroxybutyl	S-pyrrolidine	S-hydroxymethyl	S-phenyl	3-phenylbutyl	10 **	3

Table 2. Cont.

ID	Compound	Functionalities					%Inhibition (Average, n = 8)	Standard Error
	Structure	R1	R2	R3	R4	R5		
2700.012		S-4-hydroxybutyl	S-pyrrolidine	S-hydroxymethyl	S-phenyl	4-phenylbutyl	12 **	3
2700.013		S-4-hydroxybutyl	S-pyrrolidine	S-hydroxymethyl	S-benzyl	4-phenylbutyl	19 **	4
2700.014		R-butyl	S-pyrrolidine	S-hydroxymethyl	S-phenyl	4-phenylbutyl	19 **	4
2700.015		R-butyl	S-pyrrolidine	S-hydroxymethyl	S-benzyl	4-phenylbutyl	17 **	3

** *p*-Value < 0.001, * *p*-Value < 0.05. Two-Sample *t*-Test with Bonferroni-Holm Correction when compared to 2700.001. Substitutions with respect to compound 2700.001 are shown in red.

The effect of altering compound **2700.001** by making a single substitution at the R1 position was assessed. Subsequently, three analogs consisting of moving the aromatic ring further from the scaffold (**2700.002**), replacing the aromatic ring with one containing a heteroatom (**2700.006**), or by a hydroxy-substituted one (**2700.011**) were evaluated. All three compounds with a single substitution at the R1 position showed reduced inhibition levels, demonstrating the importance of the *S*-phenyl moiety in the context of compound **2700.001**. Single substitutions at the R1 position were also assessed utilizing **2700.003** as a starting point. All these R1 substitutions, **2700.007** (the aromatic ring replaced with one containing a heteroatom), **2700.009** (the aromatic ring moved further from the scaffold by inserting a methylene group), **2700.012** (the aromatic ring replaced by a hydroxy-substituted one), and **2700.014** (the aromatic ring replaced by a linear aliphatic group) (Table 2) resulted in a significant reduction in inhibition levels, further confirming the importance of the *S*-phenyl moiety in the R1 position for our lead compounds.

The effect of making a single substitution at the R4 position of **2700.001** was assessed, moving the phenyl moiety one carbon away from the scaffold. This modification significantly reduced inhibition levels (**2700.005**) (Table 2). Of note, this modification was well tolerated if made on the **2700.003** compound, when position R5 was occupied by a 4-phenylbutyl instead of the 3-phenylbutyl group present in compound **2700.004** (Table 2). Thus, the inhibitory effect of R1 single substitution of **2700.004** was also assessed. These four analog compounds, **2700.008**, **2700.010**, **2700.013**, and **2700.015**, showed significantly reduced inhibition compared to **2700.004** (Table 2). The results obtained using this set of analogs, taken together with those generated using the previous set [23], provide us insights into the sensitivity of R group substitutions and indicate the potential for further optimization with the R4 substitution of the **2700.001** and **2700.003** in future studies.

To assess the potentiating effect of amikacin by the compounds under investigation with higher accuracy, we selected those that produced inhibition levels of higher than 20% to carry out checkerboard experiments. Additionally, two compounds that inhibited at less than 20% were selected as controls (**2700.007** and **2700.013**). Then, the compounds **2700.001**, **2700.003**, **2700.004**, **2700.005**, **2700.007**, **2700.010**, and **2700.013** were tested in checkerboard assays carried out at 0, 4, 8, 16, and 32 $\mu\text{g}/\text{mL}$ amikacin and 0, 2, 4, 8, 16, and 24 μM compound. The raw experimental values obtained were adjusted using mixture modeling (described in the Section 4) to account for any compound's antimicrobial contribution to growth inhibition. These values were used to calculate the concentration of potentiated amikacin to achieve 50% and 80% bacterial inhibition of growth, the fold potentiation (over amikacin alone) of each of these dose points associated with each compound at each concentration, and the compound concentration needed to achieve 2- or 3-fold potentiation of both the 50% and 80% inhibitory dose points (Table 3 and Figure S1, Supplementary Materials). The checkerboard results indicate that the most potent inhibitor among the compounds with newly synthesized structures within the **2700** series is inferior to those already identified in the previous studies [22,23]. This includes **2700.004**, for which single-point potentiation assay results did not adequately demonstrate a difference from **2700.001**.

Molecular dynamics simulations performed on AAC(6')-Ib complexed with compound **2700.001**, as well as AAC(6')-Ib complexed with compound **2700.004**, show very similar hydrogen bond interactions. This is displayed in Table S1, which shows that the most prominent interaction in both systems, during the last 100 ns of the 400 ns runs, occurs between the compounds and the residue TYR65, followed by the residue GLN91 (Figure 2, Table S1).

A correlation study between molecular docking values and checkerboard potentiation was performed, integrating the results of the previous structure–activity relationship study [23] and the compounds presented herein. The ΔG (Kcal/mol) values were determined for the compounds across both sets for which checkerboard experiments were carried out (Table 4). Figure 3 shows a regression analysis considering the ΔG values and the compound dose required for a two-fold potentiation as determined by the checkerboard assays. The results demonstrate a significant correlation between ΔG values and inhibitory

activity ($r = 0.76$, $p = 0.0004$). The complex of compounds (**2700.001**, **2700.004**, **2700.007**, and **2700.013**) with AAC(6′)-Ib obtained from molecular docking are shown in Figure S2 (Supplementary Materials).

Table 3. Summary of checkerboard assays.

Compound ID	Inhibition (μM)			
	2-Fold		3-Fold	
	50%	80%	50%	80%
2700.001	6.5	10.4	8.8	12.9
2700.003	7.2	10.0	8.9	12.2
2700.004	19.3	23.4	>24	>24
2700.005	14.2	15.0	19.9	19.5
2700.007	>24	>24	>24	>24
2700.010	16.2	15.5	19.9	19.6
2700.013	>24	>24	>24	>24

Compound concentration needed to achieve 2- or 3-fold potentiation of the 50% and 80% inhibitory dose points.

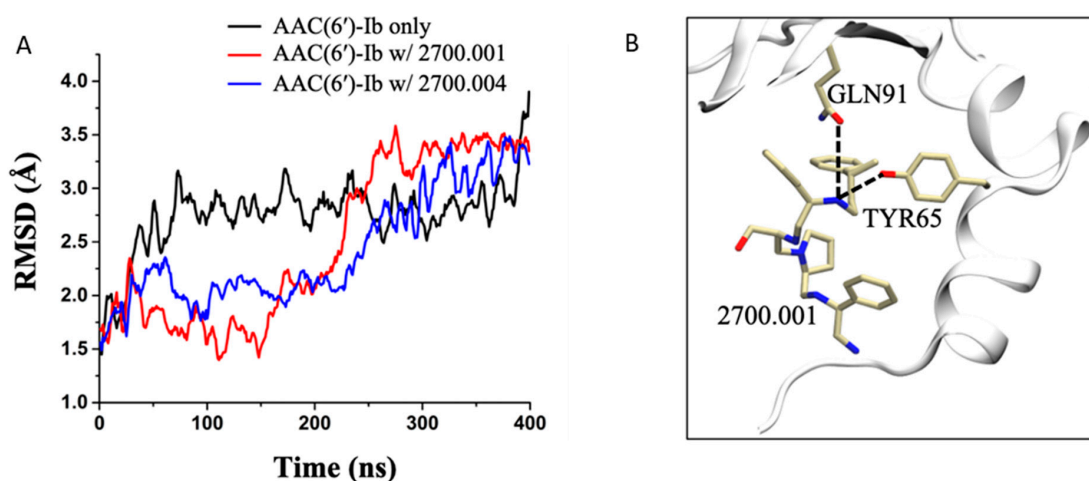


Figure 2. Molecular dynamics simulations. (A) RMSD evolution as a function of time for the AAC(6′)-Ib enzyme only (black), AAC(6′)-Ib in complex with **2700.001** (red), and AAC(6′)-Ib in complex with **2700.004** (blue). (B) 3-D representation of the hydrogen bond formation between **2700.001** and residues of the enzyme. The enzyme is shown in the cartoon representation (white), while the ligand and the important residues are shown in the stick representation.

The set of analogs analyzed in this study, in combination with the results obtained using the previous set [23], provides us insights into the sensitivity of R group substitutions. The data from this set of compounds highlight the importance of the R1 substitution of the original compound, confirm potential alterations for the R5 position, and indicate that there may still be opportunities to optimize the R3 and R4 substitutions of the **2700.001** and **2700.003** in future studies.

Low toxicity to the host is critical for any pharmacological tool. Therefore, three representative compounds, alone and in combination with amikacin, were tested HEK293 cells. Figure 4 shows that none of the three compounds tested, **2700.001**, **2700.003**, and **2700.004**, showed toxicity at concentrations up to 16 μM , alone or in the presence of 16 $\mu\text{g}/\text{mL}$ amikacin. However, compounds **2700.003** and **2700.004** at 24 μM produced significant mortality. These results show that despite the similarities among the different compounds being studied, cytotoxicity must be carefully determined in each of those that are promising inhibitors of AAC(6′)-Ib.

Table 4. Summary of compounds tested on checkerboards.

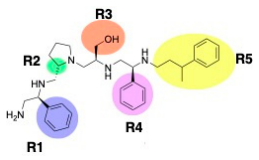
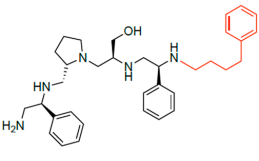
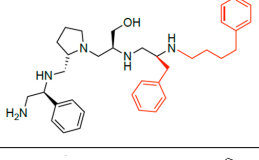
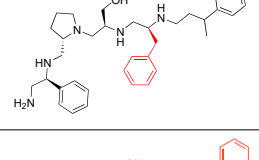
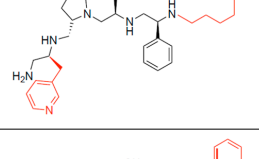
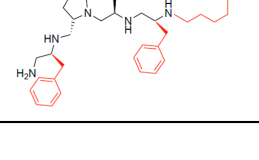
ID	Compound	Functionalities					Delta G (Kcal/mol)	Dose for 2-Fold Potentiation (μM)
	Structure	R1	R2	R3	R4	R5		
Series 2700								
2700.001		S-phenyl	S-pyrrolidine	S-hydroxymethyl	S-phenyl	3-phenylbutyl	-9.2 ± 0.6	6.5
2700.003		S-phenyl	S-pyrrolidine	S-hydroxymethyl	S-phenyl	4-phenylbutyl	-9.0 ± 0.6	7.2
2700.004		S-phenyl	S-pyrrolidine	S-hydroxymethyl	S-benzyl	4-phenylbutyl	-8.4 ± 0.2	19.3
2700.005		S-phenyl	S-pyrrolidine	S-hydroxymethyl	S-benzyl	3-phenylbutyl	-8.9 ± 0.5	14.2
2700.007		S-3-methylpyridine	S-pyrrolidine	S-hydroxymethyl	S-phenyl	4-phenylbutyl	-9.0 ± 0.4	24.0
2700.010		S-benzyl	S-pyrrolidine	S-hydroxymethyl	S-benzyl	4-phenylbutyl	-9.0 ± 0.9	16.2

Table 4. Cont.

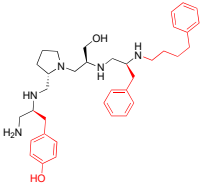
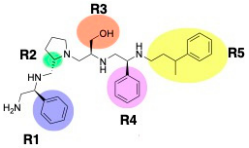
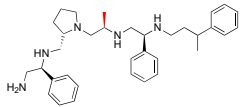
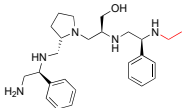
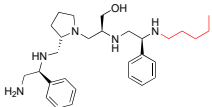
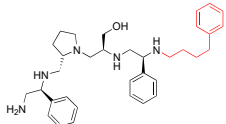
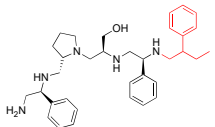
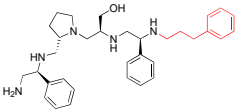
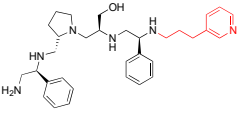
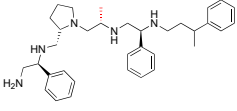
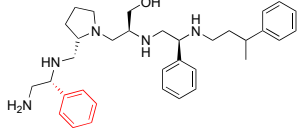
Compound		Functionalities					Delta G (Kcal/mol)	Dose for 2-Fold Potentiation (μM)
ID	Structure	R1	R2	R3	R4	R5		
2700.013		S-4-hydroxybutyl	S-pyrrolidine	S-hydroxymethyl	S-benzyl	4-phenylbutyl	-8.6 ± 0.2	24.0
Series 2637								
2637.001		S-phenyl	S-pyrrolidine	S-hydroxymethyl	S-phenyl	3-phenylbutyl	-9.2 ± 0.6	3.0
2637.004		S-phenyl	S-pyrrolidine	S-methyl	S-phenyl	3-phenylbutyl	-9.0 ± 0.3	8.7
2637.007		S-phenyl	S-pyrrolidine	S-hydroxymethyl	S-phenyl	3-ethyl	-9.6 ± 0.0	2.0
2637.010		S-phenyl	S-pyrrolidine	S-hydroxymethyl	S-phenyl	pentyl	-9.1 ± 0.5	1.7
2637.011		S-phenyl	S-pyrrolidine	S-hydroxymethyl	S-phenyl	phenylbutyl	-9.0 ± 0.6	8.3

Table 4. Cont.

Compound		Functionalities					Delta G (Kcal/mol)	Dose for 2-Fold Potentiation (μ M)
ID	Structure	R1	R2	R3	R4	R5		
2637.012		S-phenyl	S-pyrrolidine	S-hydroxymethyl	S-phenyl	2-phenylbutyl	-9.0 ± 0.4	11.1
2637.013		S-phenyl	S-pyrrolidine	S-hydroxymethyl	S-phenyl	phenylpropyl	-9.3 ± 0.5	4.1
2637.014		S-phenyl	S-pyrrolidine	S-hydroxymethyl	S-phenyl	(pyridin-3-yl)propyl	-9.4 ± 0.2	4.0
2637.019		S-phenyl	S-pyrrolidine	R-methyl	S-phenyl	3-phenylbutyl	-9.2 ± 0.1	5.4
2637.020		R-phenyl	S-pyrrolidine	S-hydroxymethyl	S-phenyl	3-phenylbutyl	-9.2 ± 0.5	5.3

Δ G (Kcal/mL) values are the binding scores obtained from molecular docking and reported as averages of the top three docking scores. For comparison, Amikacin docking gave Δ G of -8.2 ± 0.2 . Substitutions with respect to compound 2700.001 are shown in red.

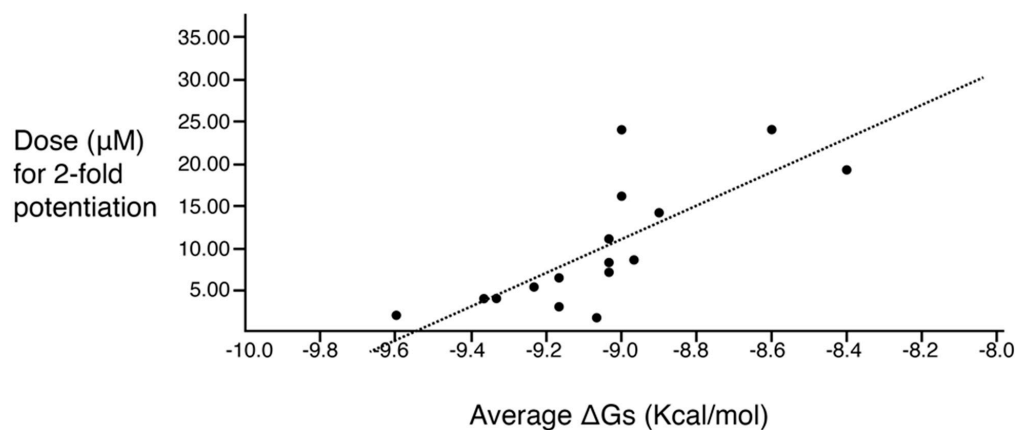


Figure 3. Predicted binding affinity vs. experimentally measured potentiation of the different compounds. The x-axis shows the calculated ΔG average when the compound interacts with the enzyme molecule. The y-axis shows the calculated efficacy for potentiation of the compounds based on the experimental data. The regression line is included in the figure. The correlation is significant ($r = 0.76$; $p = 0.0004$). The values utilized are those shown in the two rightmost columns of Table 4.

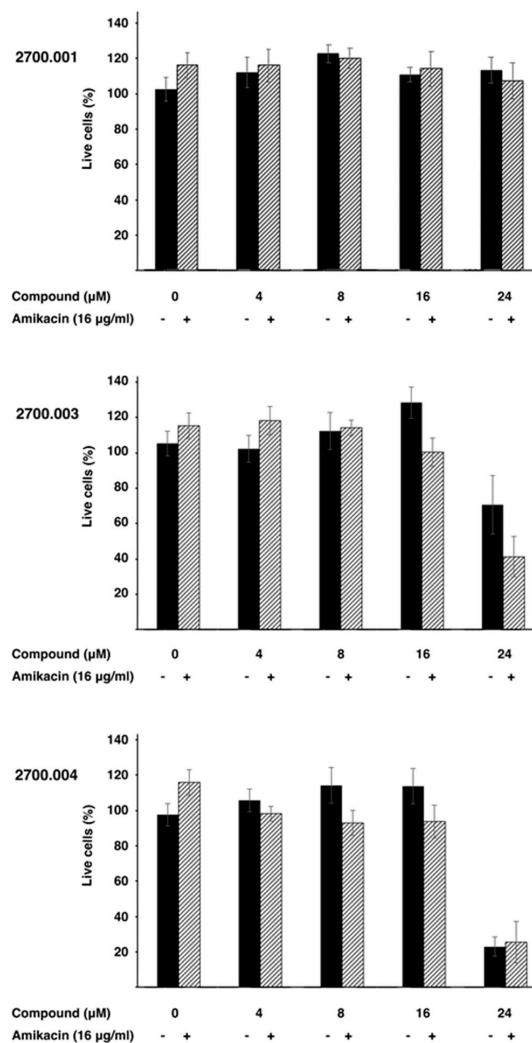


Figure 4. Cytotoxicity of compounds 2700.001, 2700.003, and 2700.004. Cytotoxicity of the compounds alone (-) or in combination with amikacin and the indicated compound (+) on HEK293 cells was assayed using a LIVE/DEAD kit as described in the Section 4.

3. Discussion

Prolonging the life of available antibiotics is crucial. Designing or discovering adjuvants that inhibit the expression or activity of biomolecules responsible for resistance can help prevent or slow the emergence of untreatable infections [1,7,30]. Such infections could increase mortality rates not only from primary diseases but also by complicating medical and dental procedures [25,31]. Although this strategy has been extraordinarily successful in expanding the usefulness of β -lactams through the combination with β -lactamase inhibitors [32], it has not yet progressed beyond research settings for aminoglycosides [25]. Since the most widespread mechanism of resistance to aminoglycosides, including amikacin, involves acetylation catalyzed by the AAC(6′)-Ib enzyme [12,16], finding inhibitors of this enzyme could allow for the treatment of numerous life-threatening infections, including those caused by carbapenem-resistant strains [20]. A proven methodology to identify bioactive compounds uses mixture-based combinatorial libraries and the positional scanning approach, which allows for the identification of scaffold structures and testing of large numbers of compounds simultaneously [22,33]. We recently identified a substituted pyrrolidine pentamine scaffold, compound 2700.001, an inhibitor of the AAC(6′)-Ib enzymatic activity [22]. This compound was used as a starting point to introduce modifications at different locations along the molecule, as well as to remove portions of the molecule, as part of SAR studies. These analyses aimed to understand the interaction between the potential inhibitors and the enzyme, as well as to identify more potent inhibitors.

In a previous study testing a series of analogs, it was concluded that the integrity of the pyrrolidine pentamine scaffold and the stereochemistry at positions R2, R3, and R4 were necessary for the compounds' ability to act as inhibitors of resistance to amikacin (Figure 1A,B) [23]. This analysis was expanded to explore the effects of additional modifications to the most active compounds identified to date (2700.001 and 2700.003). The new compounds were designed, introducing one, two, or three substitutions at the R1, R4, or R5 positions (Figure 1C and Table 1). A preliminary analysis comparing the same compounds from two independent synthesis events showed comparable results, thereby validating the findings and ensuring consistency across different synthesis batches and different biological activity determinations. Consistent with earlier results, a single substitution at the R1 position of compounds 2700.001 and 2700.003 led to a loss of inhibitory activity. Thus, the *S*-phenyl moiety remains the most effective substituent known to date for a pyrrolidine pentamine derivative to inhibit resistance. Substitutions at the R4 position of 2700.001 and 2700.003 resulted in a loss of inhibitory activity, with the only exception that replacing the *S*-phenyl group by *S*-benzyl in the compound 2700.003 produced a compound with activity comparable to that of compounds 2700.001 and 2700.003. The results obtained with the latest group of analogs suggest that it may be possible to increase the inhibitory activity, optimizing the R4 and R5 substitutions of the 2700.001 and 2700.003 compounds. Since the purpose of the single dose analysis was to pre-identify candidates having high inhibitory activity, we continued the study with checkerboard experiments. The activities of the compounds with low inhibitory activity in the single-dose experiment were confirmed by this checkerboard analysis. Among those compounds with high inhibitory activity, 2700.001, 2700.003, and 2700.004, only the lattermost did not show inhibition at high levels in the checkerboard assays. These results indicate that single-dose experiments can be an excellent pre-selection mechanism to eliminate compounds with low activity. Still, the possibility of obtaining false positives makes confirmation by checkerboard studies an essential component of the analysis. It was of interest that a regression analysis considering the molecular docking values (ΔG values) and the compound dose required for a two-fold potentiation as determined by the checkerboard assays, including all compounds tested in both this and the previous study, indicated a significant correlation between ΔG values and inhibitory activity. These results validate docking analysis as an evidentially supportive and potentially predictive tool for further modification that may result in more potent

inhibitors. The preliminary results described in this article showed that similar compounds can have different toxicity levels.

In conclusion, the results of the structure activity relationship studies indicate that those compounds with the R1–R4 substitutions present in **2700.001** but have modifications at R5 (except for 2-phenylbutyl) are candidates for further modifications at the R3 position. Although no other compound with higher inhibitory activity than the original **2700.001** has been identified, the structure–activity relationship studies have enhanced our understanding of the characteristics and effects of substituting one or more R positions. Moreover, the knowledge acquired directs future analysis to specifically focus on modifying R3, R4, and R5 positions. Overall, the progress achieved in the identification of inhibitors of acetylation mediated by AAC(6′)-Ib by mixture-based combinatorial libraries and application of the positional scanning methodology, followed by structure–activity relationship studies with the support of computational molecular modeling, together with excellent work by others to find inhibitors of resistance to a variety of antibiotics [34–36], validate the general strategy as a means to counter antibiotic resistance.

4. Materials and Methods

4.1. Bacterial Strains and Small Molecule Compounds

A. baumannii A155, a clonal complex 109 multidrug resistant strain that harbors *aac(6′)*, was isolated from a urinary sample at a hospital in the Autonomous City of Buenos Aires, Argentina [37]. Solid and liquid routine cultures were carried out in Mueller–Hinton with the addition or not of 2% agar. Cultures to determine levels of amikacin resistance to amikacin were performed in Mueller–Hinton broth. The compounds were synthesized at the Center for Translational Science at Florida International University, as described previously [22]. Briefly, a polyamide scaffold was synthesized on a solid support using standard Boc-protected chemistry. Then, the amide residues were reduced with borane, and the compounds were removed from the solid support using hydrofluoric acid (Figure S3, Supplementary Materials). The purity and identity of compounds were verified as before [23] using a Shimadzu 2020 Liquid chromatography–mass spectrometry (LCMS) system (Shimadzu, Columbia, MD, USA). Chromatographic separations were carried out on a Phenomenex Luna C18 analytical column (5 μ m, 150 mm \times 4.6 mm i.d.) with a Phenomenex C18 column guard (5 μ m, 4 \times 3.0 mm i.d.). The equipment was controlled and integrated with the Shimadzu LCMS solutions software version 5. The mobile phases A and B for LCMS analysis were LCMS-grade water and LCMS-grade acetonitrile, respectively (Sigma-Aldrich, (St. Louis, MO, USA) and Fisher Scientific (Waltham, MA, USA), both with 0.1% formic acid for a pH of 2.7). The procedure for analyzing 5 μ L aliquots was identical to that described in our previous study [23]. Figures S4 and S5 (Supplementary Materials) show the relevant information on the compounds’ characterization and degree of purification. Figure S6 (Supplementary Materials) shows the Simplified Molecular Input Line Entry System (SMILES) strings for each compound used in this study.

4.2. Initial Growth Inhibition Assays

An initial test to determine the levels of inhibition produced by the compounds was performed by measuring OD600 after 20 h of growth in Mueller–Hinton broth supplemented with 16 μ g/mL amikacin and 8 μ M of the potential inhibitor. These concentrations were selected based on previous studies using compounds with the same scaffold [22,23]. Each compound was tested in four separate experiments by duplicate. The data values, expressed in percent inhibition based on the OD600 measurements, were adjusted using the mixture-modeling described below to account for compound inhibition and averaged. The standard error of the mean for $n = 8$ percentage growth inhibition values of each compound was calculated. Each p -value for testing the difference in inhibitory activity between a compound and **2700.001** was calculated using a two-sample t -test with Bonferroni–Holm correction. A p -value of less than 0.05 was considered significant. All compounds that did

not show a substantial reduction in inhibitory activity with respect to compound 2700.001 were used in checkerboard assays.

4.3. Checkerboard Assays

Checkerboard assays were performed in Mueller–Hinton broth as described previously [22,23]. Each compound was tested on at least three independent checkerboard experiments, in which each dose combination was tested by duplicate. The variables were the potential inhibitor (tested at 0, 2, 4, 8, 16, and 24 μM) and amikacin (tested at 0, 4, 8, 16, and 32 $\mu\text{g}/\text{mL}$). Assays were carried out in microtiter plates using the BioTek Synergy 5 microplate reader (BioTek Synergy 5, Winooski, VT, USA). The data were analyzed applying an approach that quantifies exact levels of synergy, i.e., eliminating any antibacterial effect exerted by the inhibitor [22,23,38]. The model considers that amikacin and the potential inhibitors have independent antibacterial mechanisms of action. The percent activity of the mixture of the two chemicals was modeled as follows:

$$\% \text{amikacin \& compound}(x1,x2) = \% \text{amikacin}(x1) + \% \text{compound}(x2) - \% \text{amikacin}(x1) \cdot \% \text{compound}(x2) \quad (1)$$

where $x1$ and $x2$ are the amikacin and tested compound concentrations, respectively. The effective percent activity of the antibiotic alone at a given concentration, after accounting for compound activity, can be calculated using a rearrangement of the previous equation as follows:

$$\text{Eff}\% \text{amikacin}(x1) = [\text{amikacin \& compound}(x1,x2) - \% \text{compound}(x2)] / [1 - \% \text{compound}(x2)] \quad (2)$$

These calculations provide the actual change in amikacin resistance levels. The above methodology was applied to the median of the values at each dose combination. Once applied to the checkerboard data, the mean effective concentration of amikacin to achieve 50% and 80% inhibition (IC50/IC80) at each dose of the potentiating compound was determined using pairwise interpolation. The fold potentiation of amikacin for each dose of the compounds and each dose point was then calculated. Finally, the compound concentration needed to achieve 2- and 3-fold potentiation for each of the two dose points was determined using pairwise interpolation.

4.4. Molecular Docking

To prepare the receptor for docking experiments, the x-ray crystal structure of AAC(6′)-Ib complexed with kanamycin C and AcetylCoA [39] was obtained from the protein data bank (PDB 1V0C). Kanamycin C was removed from the AAC(6′)-Ib protein structure, and the final structure was converted to pdbqt format using AutoDockTools 4.2 [40]. The cavity where kanamycin C was bound to the protein was selected as the target site for virtual screening. Again, using AutoDockTools 4.2, residues W49, Y65, E73, V75, Q91, Y93, S98, D100, W103, D115, D152, and D179 were converted to flexible residues to allow for flexible binding. Next, the ligands were prepared by converting the structures of the compounds to 3D with polar hydrogen bonds and finally in pdbqt format using Open Babel 2.4.0 [41]. Molecular docking and screening were performed using AutoDock Vina 1.2 [42]. The docking scores were sorted and ranked based on their predicted binding energies (ΔG , Kcal/mol), with the lowest score representing the best binding. LigPlot+ 2.2 [43] was used to generate a 2D ligand–protein interaction map. PyMol 2.3 [44] was used for visualization and rendering.

4.5. Molecular Dynamics (MD) Simulations

All atom MD simulations were performed using the NAMD simulation package [45] for the AAC(6′)-Ib (PDB: 1V0C) enzyme as well as for the AAC(6′)-Ib in complex with compound 2700.001 and with compound 2700.004. First, the parameter and topology

files for the compounds were generated using CGENFF through the CHARMM-GUI web server [46–48]. The complexes were prepared for MD simulations using the solution builder tool in CHARMM-GUI. Each system was solvated in a cubic box of dimension $90 \times 90 \times 90 \text{ \AA}$ with TIP3P water model and neutralized by adding NaCl at 0.150 M. The resulting systems for AAC(6′)-Ib only, AAC(6′)-Ib in complex with 2700.001, and in complex with 2700.004 contained 33,230, 33,295, and 34,865 atoms, respectively. Simulations were performed with the NAMD simulation package [45] using CHARMM36m force field [49], with the temperature kept constant by using Langevin temperature coupling with a damping coefficient of 1/ps, and the pressure kept constant by using a Nose–Hoover Langevin piston [50] with a 50 fs period and 25 fs decay. All systems were minimized for 10,000 steps and equilibrated at 303.15 K and 1 atm pressure in the NVT ensemble for 250 ps at a 2 fs/step with the enzyme heavy-atoms restrained. Finally, 400 ns of unconstrained production simulations were performed with 2 fs/step for each system in the NPT ensemble. The particle mesh Ewald method [51] was used for long-range electrostatic interactions with periodic boundary conditions and a non-bonded cut-off set at 12 Å. The covalent bonds involving hydrogen atoms were constrained by ShakeH [52]. Visual molecular dynamics [53] was used to analyze the trajectories. Hydrogen bonds were calculated with a 3.5 Å distance and 30° angle cutoff.

4.6. Cytotoxicity Assays

One thousand HEK293 cells [54] per well were cultured on flat-bottom black 96 well microtiter plates for 24 h at 37 °C before addition of the test compounds and incubating for another 24 h. After this treatment, the cells were washed with sterile D-PBS, resuspended in LIVE/DEAD reagent (2 μM ethidium homodimer 1 and 1 μM calcein-AM), and incubated for 30 min at 37 °C. Fluorescence levels indicative of live (530 nm) and dead (645 nm) cells were measured. The percentage of dead cells was calculated relative to the control cells incubated with 0.1% dimethylsulfoxide. Values were obtained by averaging results from 6 to 12 repetitions. Maximum toxicity was calculated by treating cells with 70% methanol for 20 min. Results were expressed as mean ± SE. LIVE/DEAD reagent and HEK293 cells were purchased from Molecular Probes (Eugene, OR, USA) and BEI Resources (Manassas, VA, USA, catalog number NR-9313), respectively.

Supplementary Materials: The following supporting information can be downloaded at: <https://www.mdpi.com/article/10.3390/antibiotics13070672/s1>, Figure S1: checkerboard assays; Figure S2: Molecular docking; Figure S3: Synthetic method; Figure S4: Compound synthesis, purification, and characterization; Figure S5: Liquid chromatography-mass spectrometry analysis; Figure S6: SMILES strings; Table S1: AAC(6′)-Ib residues that form hydrogen bonds with 2700.001 and 2700.004.

Author Contributions: Conceptualization, M.E.T., C.P., M.A.G., R.S. and P.C.; methodology, J.S., T.T., M.S.R., H.M.D., A.J.M., T.L., Y.M., V.J., P.C., R.S., C.P., M.A.G. and M.E.T.; software, R.S. and P.C.; investigation, J.S., T.T., M.S.R., H.M.D., A.J.M., T.L., Y.M., V.J., P.C., R.S., C.P., M.A.G. and M.E.T.; resources, M.E.T., R.S., C.P., M.A.G. and P.C.; data curation, J.S., P.C., M.A.G. and R.S.; writing—original draft preparation, M.E.T., C.P., M.A.G. and R.S.; writing—review and editing, J.S., T.T., M.S.R., H.M.D., A.J.M., T.L., Y.M., P.C., R.S., C.P., M.A.G. and M.E.T.; supervision, M.E.T. and C.P.; funding acquisition, M.E.T. All authors have read and agreed to the published version of the manuscript.

Funding: This research was funded by Public Health Service grants R15AI047115 (MET) from the National Institute of Allergy and Infectious Diseases, National Institutes of Health and SC3GM125556 (MSR) from the National Institute of General Medicine, National Institutes of Health.

Institutional Review Board Statement: Not applicable.

Informed Consent Statement: Not applicable.

Data Availability Statement: Data is contained within the article and Supplementary Materials, further inquiries can be directed to the corresponding author/s.

Conflicts of Interest: The authors declare no conflicts of interest. The funders had no role in the design of the study; in the collection, analyses, or interpretation of data; in the writing of the manuscript; or in the decision to publish the results.

References

1. Boucher, H.W. Bad bugs, no drugs 2002–2020: Progress, challenges, and call to action. *Trans. Am. Clin. Climatol. Assoc.* **2020**, *131*, 65–71. [[PubMed](#)]
2. Tamma, P.D.; Aitken, S.L.; Bonomo, R.A.; Mathers, A.J.; van Duin, D.; Clancy, C.J. Infectious Diseases Society of America guidance on the treatment of extended-spectrum beta-lactamase producing Enterobacterales (ESBL-E), carbapenem-resistant Enterobacterales (CRE), and *Pseudomonas aeruginosa* with difficult-to-treat resistance (DTR-*P. aeruginosa*). *Clin. Infect. Dis.* **2021**, *72*, 1109–1116. [[PubMed](#)]
3. Centers for Disease Control and Prevention (U.S.). *Antibiotic Resistance Threats in the United States, 2019*; CDC: Atlanta, GA, USA, 2019.
4. World-Health-Organization. *WHO Bacterial Priority Pathogens List, 2024: Bacterial Pathogens of Public Health Importance to Guide Research, Development and Strategies to Prevent and Control Antimicrobial Resistance*; World Health Organization: Geneva, Switzerland, 2024.
5. McCreary, E.K.; Heil, E.L.; Tamma, P.D. New perspectives on antimicrobial agents: cefiderocol. *Antimicrob. Agents Chemother.* **2021**, *65*, e0217120. [[CrossRef](#)] [[PubMed](#)]
6. Zampaloni, C.; Mattei, P.; Bleicher, K.; Winther, L.; Thate, C.; Bucher, C.; Adam, J.M.; Alanine, A.; Amrein, K.E.; Baidin, V.; et al. A novel antibiotic class targeting the lipopolysaccharide transporter. *Nature* **2024**, *625*, 566–571. [[CrossRef](#)] [[PubMed](#)]
7. Tolmasky, M.E. Strategies to prolong the useful life of existing antibiotics and help overcoming the antibiotic resistance crisis. In *Frontiers in Clinical Drug Research-Anti Infectives*; Atta-ur-Rhaman, Ed.; Bentham Books: Sharjah, United Arab Emirates, 2017; Volume 1, pp. 1–27.
8. Krause, K.M.; Serio, A.W.; Kane, T.R.; Connolly, L.E. Aminoglycosides: An overview. *Cold Spring Harb. Perspect. Med.* **2016**, *6*, a027029. [[CrossRef](#)] [[PubMed](#)]
9. Vakulenko, S.B.; Mobashery, S. Versatility of aminoglycosides and prospects for their future. *Clin. Microbiol. Rev.* **2003**, *16*, 430–450. [[CrossRef](#)] [[PubMed](#)]
10. Houghton, J.L.; Green, K.D.; Chen, W.; Garneau-Tsodikova, S. The future of aminoglycosides: The end or renaissance? *Chem-biochem* **2010**, *11*, 880–902. [[CrossRef](#)] [[PubMed](#)]
11. Ramirez, M.S.; Tolmasky, M.E. Amikacin: Uses, resistance, and prospects for inhibition. *Molecules* **2017**, *22*, 2267. [[CrossRef](#)] [[PubMed](#)]
12. Ramirez, M.S.; Tolmasky, M.E. Aminoglycoside modifying enzymes. *Drug Resist. Updat.* **2010**, *13*, 151–171. [[CrossRef](#)]
13. Alfieri, A.; Di Franco, S.; Donatiello, V.; Maffei, V.; Fittipaldi, C.; Fiore, M.; Coppolino, F.; Sansone, P.; Pace, M.C.; Passavanti, M.B. Plazomicin against multidrug-resistant bacteria: A scoping review. *Life* **2022**, *12*, 1949. [[CrossRef](#)]
14. Labby, K.J.; Garneau-Tsodikova, S. Strategies to overcome the action of aminoglycoside-modifying enzymes for treating resistant bacterial infections. *Future Med. Chem.* **2013**, *5*, 1285–1309. [[CrossRef](#)] [[PubMed](#)]
15. Wright, G.D. Antibiotic adjuvants: Rescuing antibiotics from resistance. *Trends Microbiol.* **2016**, *24*, 862–871. [[CrossRef](#)]
16. Ramirez, M.S.; Nikolaidis, N.; Tolmasky, M.E. Rise and dissemination of aminoglycoside resistance: The *aac(6′)-Ib* paradigm. *Front. Microbiol.* **2013**, *4*, 121. [[CrossRef](#)]
17. Kawaguchi, H. Discovery, chemistry, and activity of amikacin. *J. Infect. Dis.* **1976**, *134*, S242–S248. [[CrossRef](#)]
18. Lin, D.L.; Tran, T.; Alam, J.Y.; Herron, S.R.; Ramirez, M.S.; Tolmasky, M.E. Inhibition of aminoglycoside 6′-N-acetyltransferase type Ib by zinc: Reversal of amikacin resistance in *Acinetobacter baumannii* and *Escherichia coli* by a zinc ionophore. *Antimicrob. Agents Chemother.* **2014**, *58*, 4238–4241. [[CrossRef](#)]
19. Soler Bistue, A.J.; Martin, F.A.; Voza, N.; Ha, H.; Joaquin, J.C.; Zorreguieta, A.; Tolmasky, M.E. Inhibition of *aac(6′)-Ib*-mediated amikacin resistance by nuclease-resistant external guide sequences in bacteria. *Proc. Natl. Acad. Sci. USA* **2009**, *106*, 13230–13235. [[CrossRef](#)] [[PubMed](#)]
20. Magallon, J.; Vu, P.; Reeves, C.; Kwan, S.; Phan, K.; Oakley-Havens, C.; Ramirez, M.S.; Tolmasky, M.E. Amikacin in combination with zinc pyrithione prevents growth of a carbapenem-resistant/multidrug-resistant *Klebsiella pneumoniae* isolate. *Int. J. Antimicrob. Agents* **2021**, *58*, 106442. [[CrossRef](#)] [[PubMed](#)]
21. Reeves, C.M.; Magallon, J.; Rocha, K.; Tran, T.; Phan, K.; Vu, P.; Yi, Y.; Oakley-Havens, C.L.; Cedano, J.; Jimenez, V.; et al. Aminoglycoside 6′-N-acetyltransferase type Ib [AAC(6′)-Ib]-mediated aminoglycoside resistance: Phenotypic conversion to susceptibility by silver ions. *Antibiotics* **2020**, *10*, 29. [[CrossRef](#)]
22. Tran, T.; Chiem, K.; Jani, S.; Arivett, B.A.; Lin, D.L.; Lad, R.; Jimenez, V.; Farone, M.B.; Debevec, G.; Santos, R.; et al. Identification of a small molecule inhibitor of the aminoglycoside 6′-N-acetyltransferase type Ib [AAC(6′)-Ib] using mixture-based combinatorial libraries. *Int. J. Antimicrob. Agents* **2018**, *51*, 752–761. [[CrossRef](#)] [[PubMed](#)]
23. Rocha, K.; Magallon, J.; Reeves, C.; Phan, K.; Vu, P.; Oakley-Havens, C.L.; Kwan, S.; Ramirez, M.S.; LaVoi, T.; Donow, H.; et al. Inhibition of aminoglycoside 6′-N-acetyltransferase type Ib (AAC(6′)-Ib): Structure-activity relationship of substituted pyrrolidine pentamine derivatives as inhibitors. *Biomedicines* **2021**, *9*, 1218. [[CrossRef](#)]

24. Vong, K.; Auclair, K. Understanding and overcoming aminoglycoside resistance caused by *N*-6'-acetyltransferase. *Medchemcomm* **2012**, *3*, 397–407. [[CrossRef](#)] [[PubMed](#)]
25. Magana, A.J.; Sklenicka, J.; Pinilla, C.; Giulianotti, M.; Chapagain, P.; Santos, R.; Ramirez, M.S.; Tolmasky, M.E. Restoring susceptibility to aminoglycosides: Identifying small molecule inhibitors of enzymatic inactivation. *RSC Med. Chem.* **2023**, *14*, 1591–1602. [[CrossRef](#)] [[PubMed](#)]
26. Ngo, H.X.; Garneau-Tsodikova, S. What are the drugs of the future? *Medchemcomm* **2018**, *9*, 757–758. [[CrossRef](#)] [[PubMed](#)]
27. Shakya, T.; Stogios, P.J.; Waglechner, N.; Evdokimova, E.; Ejim, L.; Blanchard, J.E.; McArthur, A.G.; Savchenko, A.; Wright, G.D. A small molecule discrimination map of the antibiotic resistance kinome. *Chem. Biol.* **2011**, *18*, 1591–1601. [[CrossRef](#)] [[PubMed](#)]
28. Blondelle, S.E.; Pinilla, C.; Boggiano, C. Synthetic combinatorial libraries as an alternative strategy for the development of novel treatments for infectious diseases. *Methods Enzymol.* **2003**, *369*, 322–344. [[PubMed](#)]
29. d'Acoz, O.D.; Hue, F.; Ye, T.; Wang, L.; Leroux, M.; Rajngewerc, L.; Tran, T.; Phan, K.; Ramirez, M.S.; Reisner, W.; et al. Dynamics and quantitative contribution of the aminoglycoside 6'-*N*-acetyltransferase type Ib [AAC(6')-Ib] to amikacin resistance. *mSphere* **2024**, *9*, e00789-23.
30. Boucher, H.W.; Ambrose, P.G.; Chambers, H.F.; Ebricht, R.H.; Jezek, A.; Murray, B.E.; Newland, J.G.; Ostrowsky, B.; Rex, J.H. White paper: Developing antimicrobial drugs for resistant pathogens, narrow-spectrum indications, and unmet needs. *J. Infect. Dis.* **2017**, *216*, 228–236. [[CrossRef](#)] [[PubMed](#)]
31. Naylor, N.R.; Evans, S.; Pouwels, K.B.; Troughton, R.; Lamagni, T.; Muller-Pebody, B.; Knight, G.M.; Atun, R.; Robotham, J.V. Quantifying the primary and secondary effects of antimicrobial resistance on surgery patients: Methods and data sources for empirical estimation in England. *Front. Public Health* **2022**, *10*, 803943. [[CrossRef](#)] [[PubMed](#)]
32. Papp-Wallace, K.M. The latest advances in beta-lactam/beta-lactamase inhibitor combinations for the treatment of Gram-negative bacterial infections. *Expert. Opin. Pharmacother.* **2019**, *20*, 2169–2184. [[CrossRef](#)]
33. Boggiano, C.; Reixach, N.; Pinilla, C.; Blondelle, S.E. Successful identification of novel agents to control infectious diseases from screening mixture-based peptide combinatorial libraries in complex cell-based bioassays. *Biopolymers* **2003**, *71*, 103–116. [[CrossRef](#)]
34. Pang, A.H.; Green, K.D.; Chandrika, N.T.; Garzan, A.; Punetha, A.; Holbrook, S.Y.L.; Willby, M.J.; Posey, J.E.; Tsodikov, O.V.; Garneau-Tsodikova, S. Discovery of substituted benzyloxy-benzylamine inhibitors of acetyltransferase Eis and their anti-mycobacterial activity. *Eur. J. Med. Chem.* **2022**, *242*, 114698. [[CrossRef](#)]
35. Punetha, A.; Ngo, H.X.; Holbrook, S.Y.L.; Green, K.D.; Willby, M.J.; Bonnett, S.A.; Krieger, K.; Dennis, E.K.; Posey, J.E.; Parish, T.; et al. Structure-guided optimization of inhibitors of acetyltransferase Eis from *Mycobacterium tuberculosis*. *ACS Chem. Biol.* **2020**, *15*, 1581–1594. [[CrossRef](#)] [[PubMed](#)]
36. Garzan, A.; Willby, M.J.; Green, K.D.; Tsodikov, O.V.; Posey, J.E.; Garneau-Tsodikova, S. Discovery and optimization of two Eis inhibitor families as kanamycin adjuvants against drug-resistant *M. tuberculosis*. *ACS Med. Chem. Lett.* **2016**, *7*, 1219–1221. [[CrossRef](#)] [[PubMed](#)]
37. Arivett, B.A.; Fiestner, S.E.; Ream, D.C.; Centron, D.; Ramirez, M.S.; Tolmasky, M.E.; Actis, L.A. Draft genome of the multidrug-resistant *Acinetobacter baumannii* strain A155 clinical isolate. *Genome Announc.* **2015**, *3*, 10–1128. [[CrossRef](#)]
38. Hoel, D.G. Statistical aspects of chemical mixtures. In *Methods for Assessing the Effects of Mixtures of Chemicals*; Vouk, V.B., Butler, G.C., Upton, A.C., Parke, D.V., Asher, S.C., Eds.; Wiley: New York, NY, USA, 1987; pp. 369–377.
39. Vetting, M.W.; Park, C.H.; Hegde, S.S.; Jacoby, G.A.; Hooper, D.C.; Blanchard, J.S. Mechanistic and structural analysis of aminoglycoside *N*-acetyltransferase AAC(6')-Ib and its bifunctional, fluoroquinolone-active AAC(6')-Ib-cr variant. *Biochemistry* **2008**, *47*, 9825–9835. [[CrossRef](#)] [[PubMed](#)]
40. Morris, G.M.; Huey, R.; Lindstrom, W.; Sanner, M.F.; Belew, R.K.; Goodsell, D.S.; Olson, A.J. AutoDock4 and AutoDockTools4: Automated docking with selective receptor flexibility. *J. Comput. Chem.* **2009**, *30*, 2785–2791. [[CrossRef](#)]
41. O'Boyle, N.M.; Banck, M.; James, C.A.; Morley, C.; Vandermeersch, T.; Hutchison, G.R. Open Babel: An open chemical toolbox. *J. Cheminform.* **2011**, *3*, 33. [[CrossRef](#)]
42. Trott, O.; Olson, A.J. AutoDock Vina: Improving the speed and accuracy of docking with a new scoring function, efficient optimization, and multithreading. *J. Comput. Chem.* **2010**, *31*, 455–461. [[CrossRef](#)] [[PubMed](#)]
43. Laskowski, R.A.; Swindells, M.B. LigPlot+: Multiple ligand-protein interaction diagrams for drug discovery. *J. Chem. Inf. Model.* **2011**, *51*, 2778–2786. [[CrossRef](#)]
44. Schrodinger, LLC. *The PyMOL Molecular Graphics System, Version 1.8*; Schrödinger, LLC.: New York, NY, USA, 2015.
45. Phillips, J.C.; Braun, R.; Wang, W.; Gumbart, J.; Tajkhorshid, E.; Villa, E.; Chipot, C.; Skeel, R.D.; Kale, L.; Schulten, K. Scalable molecular dynamics with NAMD. *J. Comput. Chem.* **2005**, *26*, 1781–1802. [[CrossRef](#)]
46. Vanommeslaeghe, K.; Hatcher, E.; Acharya, C.; Kundu, S.; Zhong, S.; Shim, J.; Darian, E.; Guvench, O.; Lopes, P.; Vorobyov, I.; et al. CHARMM general force field: A force field for drug-like molecules compatible with the CHARMM all-atom additive biological force fields. *J. Comput. Chem.* **2010**, *31*, 671–690. [[CrossRef](#)] [[PubMed](#)]
47. Jo, S.; Kim, T.; Iyer, V.G.; Im, W. CHARMM-GUI: A web-based graphical user interface for CHARMM. *J. Comput. Chem.* **2008**, *29*, 1859–1865. [[CrossRef](#)] [[PubMed](#)]
48. Lee, J.; Cheng, X.; Swails, J.M.; Yeom, M.S.; Eastman, P.K.; Lemkul, J.A.; Wei, S.; Buckner, J.; Jeong, J.C.; Qi, Y.; et al. CHARMM-GUI Input Generator for NAMD, GROMACS, AMBER, OpenMM, and CHARMM/OpenMM Simulations Using the CHARMM36 Additive Force Field. *J. Chem. Theory Comput.* **2016**, *12*, 405–413. [[CrossRef](#)] [[PubMed](#)]

49. Huang, J.; Rauscher, S.; Nawrocki, G.; Ran, T.; Feig, M.; de Groot, B.L.; Grubmuller, H.; MacKerell, A.D., Jr. CHARMM36m: An improved force field for folded and intrinsically disordered proteins. *Nat. Methods* **2017**, *14*, 71–73. [[CrossRef](#)] [[PubMed](#)]
50. Nose, S.; Klein, M. Constant pressure molecular dynamics for molecular systems. *Mol. Phys.* **1983**, *50*, 1055–1076. [[CrossRef](#)]
51. Essman, U.; Perera, L.; Berkowitz, M.; Darden, T.; Lee, H.; Pedersen, L. A smooth particle mesh Ewald method. *J. Chem. Phys.* **1995**, *103*, 8577–8593. [[CrossRef](#)]
52. Ryckaert, J.; Ciccotti, G.; Berendsen, H. Numerical integration of the cartesian equations of motion of a system with constraints: Molecular dynamics of n-alkanes. *J. Comput. Phys.* **1997**, *23*, 327–341. [[CrossRef](#)]
53. Humphrey, W.; Dalke, A.; Schulten, K. VMD: Visual molecular dynamics. *J. Mol. Graph.* **1996**, *14*, 33–38. [[CrossRef](#)] [[PubMed](#)]
54. Graham, F.L.; Smiley, J.; Russell, W.C.; Nairn, R. Characteristics of a human cell line transformed by DNA from human adenovirus type 5. *J. Gen. Virol.* **1977**, *36*, 59–74. [[CrossRef](#)]

Disclaimer/Publisher’s Note: The statements, opinions and data contained in all publications are solely those of the individual author(s) and contributor(s) and not of MDPI and/or the editor(s). MDPI and/or the editor(s) disclaim responsibility for any injury to people or property resulting from any ideas, methods, instructions or products referred to in the content.